IEEE Access
Multidisciplinary | Rapid Review | Open Access Journal

Received 21 May 2024, accepted 10 June 2024, date of publication 8 July 2024, date of current version 22 July 2024.

Digital Object Identifier 10.1109/ACCESS.2024.3424544

SURVEY

Empirical Channel Models for UAV Communication: A Comparative Study

SHI JIE SEAH[1], (Graduate Student Member, IEEE), CHEE YEN LEOW[2], (Senior Member, IEEE), RENUKA NALINGGAM[2], WEE KIAT NEW[3], (Member, IEEE), ROZANA ALAM[2], SIAT LING JONG[1], HONG YIN LAM[4], AND ABDULLAH M. ALMASOUD[5]

[1]Faculty of Electrical and Electronic Engineering, Universiti Tun Hussein Onn Malaysia, Batu Pahat, Johor 86400, Malaysia
[2]Wireless Communication Centre, Faculty of Electrical Engineering, Universiti Teknologi Malaysia, Skudai, Johor 81310, Malaysia
[3]Department of Electronic and Electrical Engineering, University College London, WC1E 7JE London, U.K.
[4]Faculty of Engineering Technology, Universiti Tun Hussein Onn Malaysia, Jalan Panchor, Johor 84600, Malaysia
[5]Department of Electrical Engineering, College of Engineering at Al-Kharj, Prince Sattam Bin Abdulaziz University, Al-Kharj 16278, Saudi Arabia

Corresponding author: Chee Yen Leow (bruceleow@utm.my)

This work was supported by the Ministry of Higher Education Malaysia through the Higher Institution Centre of Excellence (HICOE) under Grant 4J636; in part by Horizon 2020 Marie Skłodowska-Curie Actions Research and Innovation Staff Exchange (H2020-MSCA-RISE-2020) Project SwiftV2X under Grant 101008085; in part by Universiti Teknologi Malaysia (UTM) under Grant 22H33; in part by Universiti Tun Hussein Onn Malaysia (UTHM) under Grant REGG Vot No. H885 and Grant TIER 1 Vot No. Q488; in part by the Ministry of Higher Education under CRG Vot No. K262; and in part by Prince Sattam Bin Abdulaziz University under Project PSAU/2023/R/1444.

ABSTRACT Unmanned Aerial Vehicle (UAV) communications have received considerable attention in recent years as it can be applied to a wide range of applications. To expedite this development, it is essential to be able to model and accurately predict the wireless channels in UAV communication. Thus, in this paper, we compare various state-of-the-art empirical large-scale path loss models and provide quantitative insights into these models. Based on the operating frequency, environment, horizontal distance, and altitude, we recommend the suitable choice of empirical models for UAV communication. These insights not only facilitate more practical theoretical studies but also motivate measurement campaigns in the future.

INDEX TERMS Air-to-ground (AG) propagation, empirical path loss model, ground-to-air (GA) propagation, unmanned aerial vehicle (UAV).

I. INTRODUCTION

In recent years, Unmanned Aerial Vehicle (UAV) has gained significant interest in the field of wireless communication due to its three-dimensional (3D) mobility, deployment flexibility, and compatibility with a wide range of applications [1]. In general, a UAV can be used as an aerial-based station, aerial relay, or aerial server to serve networking devices efficiently. On the other hand, a UAV can be used as an aerial user to perform arbitrary missions such as precision agriculture, construction, delivery, and monitoring. These capabilities enable UAV communication to find a wide range of applications that are crucial in the future 6th Generation (6G) wireless networks [2].

UAVs can be used for a wide range of purposes that are advantageous to both UAV users and corporations. UAVs can serve as base stations, extending a wireless network to locations that might not otherwise have access to one [3], [4], [5]. This can be particularly useful in disaster-stricken areas where communication networks may have been damaged. UAVs can be used as communication network relays to increase the reach of networks and improve coverage in remote areas [6], [7]. The employment of UAVs in various industries, including agricultural, infrastructure inspection,

The associate editor coordinating the review of this manuscript and approving it for publication was Jiayi Zhang.

and environmental monitoring, can be advantageous to UAV users [8], [9], [10]. UAVs can also gather data fast and effectively, giving companies useful information to help them optimise their operations. Additionally, UAVs can be used for search and rescue operations, delivery services, and military and defence operations [8], [11], [12], [13]. As technology continues to improve, we can anticipate seeing even more innovative use cases for UAVs that can benefit both individuals and corporations.

Nevertheless, the altitude of the UAV could lead to several drawbacks. In particular, the Aerial Base Station (ABS) may engender strong Line-of-Sight (LOS) interference to many other base stations in the downlink due to its wide coverage. In the uplink situation, an ABS might suffer strong interference from many terrestrial user equipment due to the LOS links. In contrast, the aerial user suffers strong LOS interference from many terrestrial base stations in the downlink, while in the uplink, the aerial user creates interference to many other user equipment. In addition, the 3D mobility of the UAV may create a time-varying wireless channel. Specifically, the channel parameters would frequently change with time and space leading to unreliable communications [14]. In certain scenarios, the transmitted signal undergoes multiple reflections, scattering, and diffractions as it traverses the scattering region surrounding the transmitter and receiver. Consequently, a double-scattering channel model and UAV selection scheme considering the impact of shadowing effects was introduced in [15] to characterise the behaviour of the received signal in UAV-enabled communication.

To improve the network performance, it is thus essential to model and accurately predict the wireless channel for UAV communication. In the context of communication systems and signal processing, channel models can be neatly categorised according to their defining characteristics. The variation of the wireless channel can be generally divided into two types of fading: large-scale fading and small-scale fading [16]. The large-scale fading is due to the signal attenuation as a function of path distance, altitude, and shadowing. The small-scale fading is due to the constructive and destructive combination of the multiple signal paths at the receiver. The large-scale and small-scale fading can be represented by deterministic, statistical, empirical, and hybrid channel models. Deterministic models are usually obtained directly from analysing the propagation paths of electromagnetic wave, for example the Friis's free space path loss model, log distance path loss model, two-ray ground reflection model [17], etc. Ray tracing [18] is also categorised as deterministic model where it is derived by incorporating physical principles and geometrical considerations to model the propagation of signals through the environment. Statistical distribution-based models are designed to represent generalised behaviors or trends in a system based on theoretical mathematical equations and probability distributions. Common statistical distributions include Rayleigh, Rician, and Nakagami-m for small scale fading [19], [20]. Probabilistic based models such as Probabilities of LOS and NLOS [21], [22], map-based LOS and NLOS model [23], [24], topographic featured based LOS and NLOS model [25] are commonly used to capture the likelihood of LOS and NLOS channel as a function of UAV altitude, position and operating environment. The LOS large-scale path loss models employed in these models [19], [20], [21], [22], [23], [24], [25] are mainly based on the theoretical free space path loss model or the generic distance path loss model with environment or UAV height dependent path loss exponent. On the other hand, empirical large-scale path loss models such as 3GPP [26], ITU-R [27], COST-Hata modified [28] are derived from direct observations or measurements in real-world scenarios. Meanwhile, a hybrid channel model combines elements of different modelling approaches, typically empirical and deterministic, to provide a more comprehensive representation of real-world wireless communication channels. For instance, a hybrid method which consists of statistical and deterministic model was used in [29] for low Terahertz UAV communication. In this paper, we mainly focus on the empirical large-scale path loss models for UAV communication which are useful to determine the average channel gain between UAV and ground node. Empirical path loss models can be readily integrated with existing small-scale fading models or probabilistic/deterministic LOS and NLOS models to capture the instantaneous channel gain. The integration of large-scale and small-scale fading models is beyond the scope of this paper.

In general, path loss (PL) in UAV communication can be classified into three types of radio propagation: Air-to-Ground (AG) propagation, Ground-to-Air (GA) propagation, and Air-to-Air (AA) propagation. For ease of expositions, we classified the AG, GA, and AA propagation as the aerial links, while the ground-to-ground (GG) propagation is referred to as the terrestrial link. It is worth noting that these propagations as well as their characteristics are highly distinctive in the real-world environment. The researchers in [30] acknowledged that traditional channel models may not be suitable for low-altitude UAV applications due to the unique characteristics of the environment, prompting them to conduct a measurement campaign in a scenario featuring metal containers, buildings, and trees. The impact of UAV altitude and distance on the simplified dual slope path loss model was analysed. In [31], a stochastic modelling approach to investigate the impact of UAV altitude and optimal placement of the ground receiver on path loss for both static and mobile UAVs was studied in both open-field and suburban scenarios. Based on the measured values, a modified free space path loss model is proposed, incorporating both link distance and height factors. The empirical model presented in [32] is formulated by enhancing the fundamental coefficients such as the path loss exponent and height-dependent factors, based on the channel model in the 3GPP TR 38.901 framework. In addition to studying environmental characteristics, the literature also examines propagations related to various applications,

such as wireless sensor networks [33], [34], [35] and IEEE 802.11 networks [36], [37].

Although several empirical measurement campaigns have been carried out to capture the large-scale path loss for UAV communication [28], [38], [39], [40], [41], [42] in specific environments, the established existing empirical models have not been directly compared as they are developed independently based on the measurement results. Several survey papers review the existing UAV communication channel models [43], [44], [45] and provide general and qualitative comparisons of the existing empirical large-scale path loss models. However, there remains a notable gap where there is no comprehensive quantitative comparison of all applicable existing empirical models based on common parameters. Quantitative comparison of existing empirical models is not only important to assess the performance and suitability of the models for the target environments and scenarios but also serves as guidelines for model selection.

Motivated by these gaps, this paper undertakes a systematic examination of recent empirical models for UAV communications. Our goal is to offer a comprehensive comparison, quantitative analysis, and informed suggestions for selecting the most suitable empirical models based on operating frequency, environment, UAV's horizontal distance, and UAV's altitude. These findings help to enhance the precision of wireless channel prediction, enable more practical theoretical research, and guide future measurement campaigns in UAV communication. The impactful contributions of this paper are summarised as follows:

- The key differences between terrestrial and aerial links are identified. Unlike existing works, we further consider the end-to-end propagation, excessive attenuation caused by the environment, the UAV's characteristics as well as the transmitter and receiver antenna settings.
- Next, we gather a comprehensive list of relevant empirical models, outlining their measurement setup and considerations. The models are simulated based on common parameters to enable fair comparison and the key parameters that influence these path loss models are analysed in detail.
- Depending on the operating frequency, environment, UAV's horizontal distance, and UAV's altitude, we provide recommendations for suitable empirical path loss models for UAV communication accordingly. This not only provides a guideline for selecting the empirical model depending on target applications, but it also facilitates more practical theoretical studies.
- Lastly, we provide insights on the path loss value of different empirical models and compare different path loss models quantitatively over different network parameters and settings. This allows us to further understand the discrepancy and limitations of existing empirical models as well as motivate measurement campaigns in the future.

In summary, this study addresses a major gap in the field of UAV communication by providing a comprehensive examination of empirical path loss models. We contribute significantly to the further development of wireless channel prediction precision, theoretical advancements, and strategic planning of measurement campaigns by identifying the complexities of aerial and terrestrial link characteristics, documenting existing models, providing corresponding suggestions, and delivering quantitative insights.

The rest of the paper is organised as follows: Section II presents the UAV communication background, while the key differences between terrestrial and aerial links are discussed in Section III. Section IV reviews the empirical channel models, and Section V provides the numerical results. Finally, the conclusions are made in Section VI.

II. BACKGROUND OF UAV COMMUNICATION

UAVs have been extensively used for military purposes for over thirty years [46]. Recently, UAVs have gained attention in civil applications, such as search and rescue operations, transportation management, construction, medical care, agriculture, wildlife monitoring, package delivery, photography, structural inspection, and many other applications. UAVs can be classified into fixed-wing and rotary-wing depending on the type of wings and also can be classified into High-Altitude Platforms (HAP) and Low-Altitude Platforms (LAP) depending on the flying altitude [47]. HAPs are typically quasi-stationary and deployed at altitudes above 10 km above the earth [47], [48], while LAPs are deployed at altitudes below 10 km [48].

UAVs have the benefits of high manoeuvrability, dynamic positioning, rapid deployment, low maintenance, and operating costs. These benefits make them a perfect fit for wireless communications. First, UAVs can be equipped with radio communication devices to function as aerial users which connect to the terrestrial communication network for command and control and data streaming. Second, UAVs can be deployed as ABSs to support emergency or temporary communications or provide access to remote areas. Third, UAVs can also be used as airborne wireless relays to extend the terrestrial base stations' coverage and capacity. In addition, a group of UAVs can also be deployed as a flying swarm to coordinate and contribute to a specific task. Furthermore, the 3rd Generation Partnership Group (3GPP), since its release on 15 dated March 2017 [26], has initiated the study item definition of enhanced LTE support for aerial users to identify the UAV wireless communication challenges and promising solutions to overcome them. Several leading telecommunication companies have begun practical implementation of UAV communications to take advantage of this emerging technology. For instance, AT&T has developed cell-on-the-wing to provide LTE coverage to ground users. Nokia Bell laboratory has also developed F-cell (flying small cell) to set up aerial small cells while Verizon has initiated the ALO (Airborne LTE Operations) project to provide in-flight cellular connectivity [49]. Moreover, authors in [50] have proposed a drone-assisted hierarchical two-layered network connected to

5G with the placement of UAV as relays in 3D to offer Voice over WiFi (VoWiFi) service to users on the ground.

In addition to the benefits of UAV communication, the aerial link has unique channel characteristics that differ from the terrestrial link. UAV communication is inherently 3 dimensional (3D) and supports rapidly reconfigurable communication for a relatively shorter duration, e.g., a few minutes or hours. In contrast, conventional terrestrial communication is two-dimensional (2D) and supports long-term deployment to facilitate communication between ground nodes only [47]. Compared to the conventional terrestrial base station, UAV can establish more reliable communication by adjusting its altitude to create a strong LOS link and efficiently reduce the required transmit power. Nevertheless, the aerial link can be affected by airframe shadowing, UAV wobbling, and noise from the UAV's electrical and mechanical components [44]. The distribution of multipath components, the UAV's size, shape, material, and surface structure can also affect the aerial link. In addition, the operating frequency, antenna position on the UAV, antenna type, orientation, polarisation, and beamforming in a Multi-Input and Multi-Output (MIMO) system can substantially affect the aerial link as well.

Furthermore, the UAV may establish strong LOS links to multiple terrestrial base stations, which could cause severe interference to other terrestrial users during the uplink communication from the UAV to the ground station [51]. Aerial users hovering at the cell edge also suffer from frequent handovers due to multi-cell interference. The other way around, downlink communication between the ground station and UAV can be affected by the interference caused by neighbouring ground stations communicating with the ground and/or aerial user [11], [52]. Doppler shift and delay spread must be considered while the UAV moves at a more significant speed [53], [54].

Moreover, the ground communication system is engineered mainly to facilitate the ground users. This is done by down tilting the antenna's main lobe to the ground users. Consequently, the connected aerial users only receive coverage through the antenna's side lobe. Thus, understanding the channel prior to wireless system design is essential in UAV communication. This necessitates a comprehensive study on the radio propagation of UAV communication and the most critical factors owing to its changes.

III. KEY DIFFERENCES BETWEEN TERRESTRIAL LINK AND AERIAL LINK

In general, aerial link exhibits different characteristics compared to conventional terrestrial links. In GG propagation, obstacles are usually present in LOS propagation. This brings the disadvantage of higher transmit power in the terrestrial link compared to the aerial link. Furthermore, due to the UAV's altitude, motion, and velocity, the variation of the aerial link is much more rapid than that of the terrestrial link. Another key characteristic is the location and placement of the antenna. Specifically, in GG propagation, the placement

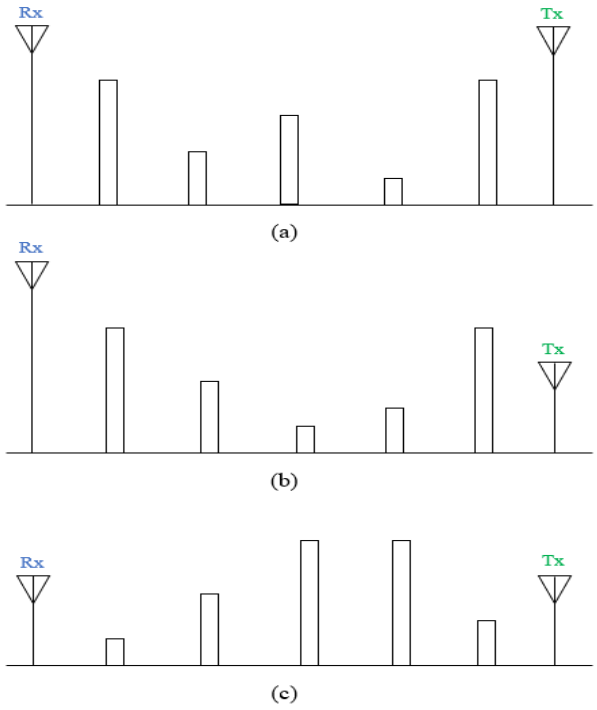

FIGURE 1. The scenarios of possible antenna placement for terrestrial propagation [64].

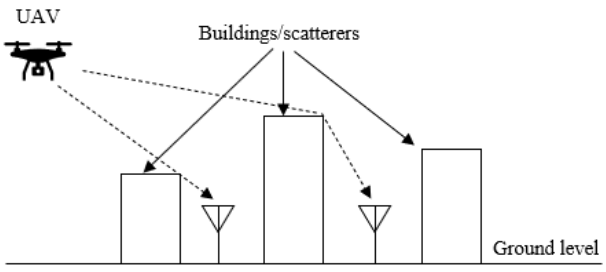

FIGURE 2. The scenarios of air-to-ground propagation [55].

of the antenna can be classified into three cases as shown in Figure 1: (a) both the transmitter (Tx) and receiver (Rx) antennas are placed above rooftop or obstacles, (b) one of the antennas is placed higher than the other and above the rooftop or obstacles, and (c) both antennas are placed below the rooftop or obstacles. Figure 2 illustrates the communication of the AG propagation where a UAV is flying in the air and an antenna is placed on the UAV while the other antenna is on the ground. In AG propagation, the radio waves travel freely without obstacles in the free space for a large distance before reaching the man-made structures on the ground [55]. In contrast, in GA propagation, parts of the radio waves propagate around man-made structures before reaching the receiver in the air. The man-made structures are referred to as the buildings or signboards as well as the flyover that would cause scattering and diffraction of the signal and subsequently lead to severe attenuation. For AA propagation, the communication link is set up between multiple UAVs together with the Tx and Rx antenna placed on each UAV in the air. It is often

modelled using the free-space path loss model due to fewer obstacles in the air and negligible reflection on the ground, and thus its discussion is omitted from this paper.

There are several factors that would affect the performance of the aerial link. The frequency band is one of the most fundamental factors. The L-band and C-band are the typical frequency bands that have been previously researched [40], [41], [42], [56]. It is important to note that the channel would suffer higher path loss attenuation as the frequency increases. Another factor is the environment. It is observed that the climate or changes in weather would lead to additional attenuation to the propagation. For instance, the ground surface temperature, air temperature as well as humidity would affect the signal strength in the radio wave propagation [57]. On top of that, the type of terrain also plays an important role in the propagation of the aerial link. According to the International Telecommunication Union Recommendation (ITU-R) P.1411-11 [27], there are five types of environments: very high-rise, high-rise, suburban, residential, and rural. The usage of the mobile terminal, antenna position, as well as the heights, and the structure of buildings in these environments are generally different. The definition and concerns of each environment have been detailed in [27]. The use of the antenna is another factor that affects the aerial link. The properties of the antenna, such as its type, orientation, and the number of antennas, are important in determining the performance of the aerial link. The most popular antenna orientation used in vehicular communication applications is omni-directional due to its good performance during motion [37], [58]. In UAV communication, directional and omni-directional antennas are frequently used [59], [60], [61], [62], [63]. As reported in [63], shadow fading is observed and decreases with the increase of flight height when the omni-directional antenna is considered. However, the use of directional antenna does not reduce the shadow fading with increasing flight height due to the impact of sidelobes of the directional antenna. This means that the choice of antenna types and orientation used in a UAV measurement campaign depends on the flight height.

IV. REVIEW OF UAV EMPIRICAL PATHLOSS MODELS

A comprehensive understanding of the mathematical modelling of the wireless channel is very important because it facilitates a more accurate prediction of system performance and provides the mechanism to test and evaluate methods to see the effects caused by radio propagation.

The following approaches are surveyed to find the empirical models that best suit the UAV aerial link characteristics. Firstly, we identify the existing empirical path loss models that can be applied to UAV communication based on models' assumptions and settings such as operating frequency, environment, UAV's horizontal distance, and UAV's altitude. Secondly, we analyse the key factors that affect the path loss model. Finally, we review these existing models and highlight the research gaps in existing empirical path loss models.

A. EMPIRICAL PATH LOSS MODELS

To find the most relevant propagation models for UAV communication, we focus on frequently studied and most common deployment scenarios. The selected models in this paper are suitable for AG and GA propagation in the outdoor deployment while AA propagation is omitted due to its similarity to free space path loss. Furthermore, the empirical models are shortlisted based on the parameters, assumptions, and settings. The relevant parameters are the operating frequency, environment, UAV's horizontal distance, and UAV's altitude. Note that, the UAV may serve as a transmitter or receiver.

The following is a list of the shortlisted empirical path loss models:

1) 3GPP TR 36.777 MODEL

The Third Generation Partnership Project (3GPP) is an industry-driven consortium that standardises cellular technology. The 3GPP has been actively identifying the requirements, technologies, and protocols for aerial communications. The 3GPP studied the use of enhanced Long-Term Evolution (LTE) support for aerial vehicles and successfully released Technical Report TR 36.777. The release contains the results and findings from the study item ''Study on Enhanced Support for Aerial Vehicle''. The purpose of this release is to identify the performance of Release-14 LTE networks when used to serve aerial vehicles like drones and to document the performance-enhancing solutions to optimise the LTE connectivity for aerial vehicles [26].

2) ITU-R.P.1411-11 MODEL

This ITU-R recommendation provides guidance on short-range outdoor propagation over 300 MHz to 100 GHz. Information is given on basic transmission loss models for LOS and Non-Line-of-Sight (NLOS) environments, building entry loss, multipath models for both environments of the street canyon and over rooftops, number of signal components, polarisation characteristics, and fading characteristics. This recommendation can also be used in compatibility studies. The propagation model is symmetric in the sense that radio terminals at both ends of a path are treated in the same manner. From the model's perspective, it does not matter which terminal is the transmitter and which is the receiver. Thus, the model is applicable for AG and GA deployment. Buildings and trees are the primary attenuation factors for propagation over a path length of less than 1000 m. This is typically found in an urban and suburban environment where the effect of the building is predominant. Basic transmission loss coefficients for above-rooftop propagation provided in the ITU document [27] are considered.

3) COST HATA MODIFIED MODEL

The COST Hata modified model was developed based on an AG measurement campaign [28]. The measurement

campaign considers two operating frequencies, in particular, 785 MHz and 2160 MHz. In this campaign, the UAV serves as a transmit ABS. The transmit ABS was installed with two antennas, and it hovers at various altitudes ranging from 50 to 950 m while the receiver was installed on the top of a mobile SUV-type vehicle. The path loss was measured from the ABS to the vehicle. Furthermore, the campaign considers urban, suburban, and rural environments with a horizontal distance of up to 70000 m from the projection of the ABS at the ground.

4) 3GPP TR38.901 MODIFIED MODEL

Similarly, a measurement campaign was conducted for AG propagation to develop the 3GPP TR 38.901 modified model [38]. Compared to other works, this campaign was sounded at 919 MHz and 2412 MHz. In the former, i.e. 919 MHz, a rural environment was considered, whereas, in the latter, i.e. 2412 MHz, an urban environment was considered. For the rural environment, the UAV flies from 1000 m to 10000 m horizontally away from the terrestrial base station, while for the urban environment, the UAV flies from 145 m to 450 m horizontally away from the terrestrial base station. In these two environments, the UAV flies at different altitudes ranging from 25 m to 150 m. The transmit UAV is equipped with two omni-directional antennas while the receiver on the ground was installed on top of a five-storey building to emulate the terrestrial BS. The path loss was measured from the UAV to the terrestrial BS.

Two key characteristics are observed in this campaign. Firstly, in the urban environment, the path loss increases with distance which is consistent with the terrestrial link. Nevertheless, there is a discrepancy between the path loss of the aerial link and that of the terrestrial link for the same total distance, which implies that the UAV's horizontal distance and the UAV's altitude affect the path loss substantially. Secondly, in a rural environment, the path loss experiences a discrepancy at about 4000 m horizontal distance. Due to these characteristics, a correction factor is proposed to improve the accuracy of 3GPP TR 38.901 for the aerial user. The correction factor is optimally obtained by fitting the data with the Minimum Mean Square Error (MMSE) criterion [38].

5) AMORIM MODEL

The Amorim model is another interesting path loss model for AG propagation [39]. This model was developed using the LTE networks, which operate at 800 MHz and is suitable for hilly terrain in rural areas. Unlike the above models, this model aims to identify the path loss exponent and shadowing effects for AG propagation with respect to the UAV's altitude. Therefore, in this model, a height-dependent parameter is introduced. Nevertheless, the UAV's altitude is only measured up to 120 m. In this model, it is observed that the path loss and shadow fading effects become milder as the UAV's altitude increases.

TABLE 1. Empirical path loss models in UAV communication: settings and considerations.

Empirical PL Model	Environment	Applicability Ranges
3GPP TR36.777	Urban Suburban Rural	f = 800 MHz & 2000-2600 MHz h_{UAV} = 10-300 m (rural) & 22.5-300 m (urban and suburban) h_{GS} = 25 m,10 m & 35 m Horizontal distance = d_{2D} ≤10000 m (rural) & d_{2D} ≤4000 m (urban & suburban)
ITU-R P. 1411-11	Urban Suburban	f = 2200-73000 MHz h_{UAV} = Not specified h_{GS} = Not specified Horizontal distance = 55-1200 m
COST Hata Modified	Urban Suburban Rural	f = 785 MHz & 2160 MHz h_{UAV} = 30-1000 m h_{GS} = 2.30 m Horizontal distance = Max 70000 m
3GPP TR38.901 Modified	Urban Rural	f = 919 MHz & 2412 MHz h_{UAV} = 50-150 m h_{GS} = 28 m Horizontal distance = 145-320 m (urban) & 1000-10000 m (rural)
Amorim	Rural	f = 800 MHz h_{UAV} = 120 m h_{GS} = 1.5 m Horizontal distance = 1000-22000 m
Matolak	Urban Suburban Rural	f = 960 MHz & 5060 MHz h_{UAV} = 504 m and above h_{GS} = 20 m Horizontal distance = 720-46000 m

6) MATOLAK MODEL

In 2013, the National Aeronautics and Space Administration (NASA) Glenn Research Center supported an AG channel measurement campaign [40], [41], [42], which subsequently led to the emergence of the Matolak model. In this campaign, the AG channel measurements are taken in both L- and C-bands near-urban areas in Cleveland, Ohio, and in suburban areas in Cleveland, Ohio; Palmdale, California; and Latrobe, Pennsylvania. The transmit antennas were fixed at 20 m above the ground, and the receive antennas were mounted on the bottom of an S-3B aircraft that flew from 500 m to 1000 m above the ground. By using the log-distance linear fit as the reference, the suburban/near-urban path loss exponent ranges from 1.5 to 2.0 with a standard deviation of less than 3.2 dB. It is worth noting that the exponent value is less than 2.0 in this model due to the effect of the aircraft antenna in short distances. Table 1 shows the summary of the existing empirical path loss models in UAV communications.

B. KEY PARAMETERS IN THE EMPIRICAL MODELS

1) 3GPP TR 36.777 MODEL

The considered environments in the 3GPP TR 36.777 model are Urban Macrocell (UMa), Suburban Microcell (UMi),

TABLE 2. The coefficients in ITU-R P.1411-11 model.

Frequency range (MHz)	Distance range (m)	α	β	γ	σ
2200-73000	55-1200	2.29	28.6	1.96	3.48

TABLE 3. The coefficients in cost hata modified model.

PL Models		a_1	a_2	a_3	a_4	a_5	b	$d_{BK}(m)$	$d_{CF}(m)$	$h_{CF}(m)$
Territorial channel	Hata model	69.55	26.16	13.82	44.9	6.55	-	-	-	-
	COST-2100	46.3	33.9	13.82	44.9	6.55	-	-	-	-
A2G channel	our model (UHF)	46.39	26.16	15	44	0.8	0.84	2000	60000	1000
	our model (S)	20.18	33.9	13.6	53.78	1.16	1.16	2000	20000	1000

and Rural Macrocell (RMa). Their path loss is computed in (1), (2), and (3), as shown at the bottom of the next page, respectively. d_{3D} is the 3-dimensional distance in meters, f_c is the centre frequency of the signal in MHz, and h_{UAV} is the UE altitude in meters (m).

2) ITU-R.P.1411-11 MODEL

The ITU-R P.1411-11 provides guidance on outdoor short-range propagation over the operating frequency range from 2200 MHz to 73000 MHz. The path loss in the LOS environment is expressed in (4), as shown at the bottom of the next page, and the coefficients of the path loss model are presented in Table 2.

3) COST HATA MODIFIED MODEL

In [28], an empirical path loss model was proposed for aerial links based on the COST-2100 specification. This extends the COST Hata model. Based on the channel measurement results, the authors consider the operating frequency, the UAV's horizontal distance, and the UAV's altitude. The path loss in unit decibels (dB) is given in (5)-(8), as shown at the bottom of the next page. The f'_{COST} is originally defined in the COST-2100 model. However, the parameters in (6) are modified based on the AG channel measurement results. Furthermore, Δ_{CF} (h_{BS}) is a correction factor to reflect the effect of the ABS's altitude, f_c is the operating frequency in MHz, h_{BS}, and h_{UAV} are respectively the altitude/height of ABS and UE in metres, and d_{2D} is the horizontal distance in metres. In addition, d_{BK} is the breaking point of the horizontal distance whereas a_1 to a_5 are the adjusted coefficient values. Besides, d_{CF} is the cutting-off applicable distance range, and h_{CF} is the cutting-off ABS altitude of the model. The coefficients of the COST Hata modified model are summarised in Table 3.

4) 3GPP TR 38.901 MODIFIED MODEL

By leveraging the correction factor, the PL for the UMa environment with an altitude above 25 metres ($h_{UT} \geq 25$ metres) is computed in (9)-(10), as shown at the bottom of the next page. The correction factor depends on the UAV's altitude, and it is proposed as given in (11), as shown at the bottom of the next page. In (9), d_{3D} is the 3-dimensional distance in metres, f_c is the operating frequency in MHz, and h_{UAV} is the UAV's altitude in metres. PL_{UMa}^{3GPP} is the terrestrial path loss defined by the 3GPP model for the UMa scenario (i.e., reference), and CF_{UMa} is the correction factor relevant to the altitude of the aerial user.

TABLE 4. The coefficients in amorim model.

Parameter	p_1	p_2
α	3.9	-0.9
β	-8.5	20.5
σ	8.2	-2.1

Similar to the UMa scenario, a new path loss model is proposed in the RMa environment based on the 3GPP TR 38.901 model. Due to the existence of the breaking point, a two-segment function with respect to the horizontal distance is adopted. It is worth highlighting that the path loss did not show variation with respect to the UAV's altitude. Thus, the correction is independent of the UAV's altitude, which is different from the UMa environment. In particular, the path loss in the RMa environment is expressed in (12)-(14), as shown at the bottom of the next page. PL_{RMa}^{3GPP} is the terrestrial path loss defined by the 3GPP model for the RMa environment and CF_{RMA} (d_{2D}) is the correction factor that is relevant to the UAV's horizontal distance. In (13), as shown at the bottom of the next page, h_{Blg} is the average building height in the surrounding environments, and in the measurement campaign, h_{Blg} is set to 5 metres. Considering the breaking point at a horizontal distance of 4000 m, the correction factor is modelled by a two-segment function as given in (14) where d_{2D} is measured in metres.

5) AMORIM MODEL

As discussed, [39] proposes a height-dependent channel model. In particular, the path loss is computed according to (15) whereas its channel parameters are given in (16)-(18). In (15), PL_{Amo} represents the path loss, p is the constant value for each height-dependent parameter, and its value is given in Table 4. h_u is the UAV height. The height, h_{FSPL} can be calculated using generic free space model given in free space path loss model as (20) when the free space propagation is

assumed and $\alpha = 2.0$.

$$PL_{Amo} = \alpha 10\log_{10}(d) + \beta + X_\sigma \quad (15)$$
$$\alpha(h_u) = max\left(p_{\alpha_1} + p_{\alpha_2}\log_{10}(h_u), 2\right) \quad (16)$$
$$\beta(h_u) = p_{\beta_1} + p_{\beta_2}\log_{10}(min(h_u, h_{FSPL})) \quad (17)$$
$$\sigma(h_u) = p_{\sigma_1} + p_{\sigma_2}\log_{10}(min(h_u, h_{FSPL})) \quad (18)$$

6) MATOLAK MODEL

In the Matolak model, the modified log-distance path loss models are employed to measure the path loss. Specifically, the path loss is expressed in (19) as follows:

$$PL(R) = A_0 + 10n\log\left({}^{R}/_{R_{min}}\right) + X + \varsigma F_A \quad (19)$$

where $R_{min} \leq R \leq R_{max}$, A_0 is the constant attenuation at the minimum link distance, n is the path loss exponent, $\varsigma = -1$ accounts for UAV travelling toward the terrestrial base station, and $\varsigma = +1$ accounts for UAV travelling away from the terrestrial base station, F_A is a small (positive) adjustment factor for the travelling direction of the UAV, and X is a zero-mean Gaussian random variable with a standard deviation of σ. Table 5 further presents the constant coefficients of this model.

7) FREE SPACE PATH LOSS (FSPL) MODEL

The FSPL is considered for benchmarking purposes. The FSPL is used by some existing theoretical studies. Free-space model is a baseline model that provides a measure of PL when the transmitter and receiver are within line-of-sight (LOS) range without any obstacles between them. It is based on the Friis' free-space transmission equation, given in the logarithmic domain in (20) as follows:

$$FSPL\,[dB] = 20\log_{10}(f_c) + 20\log_{10}(d) - 27.55 \quad (20)$$

where d is the distance between the transmitter and the receiver in m, and f_c is the frequency in MHz.

$$\text{Urban} = 20\log_{10}\left(\frac{f_c}{1000}\right) + 22\log_{10}(d_{3D}) + 28 \quad (1)$$

$$\text{Suburban} = max\left(20\log_{10}\left(\frac{d_{3D}}{1000}\right) + 20\log_{10}\left(\frac{f_c}{1000}\right) + 92.45, 30.9 + \left(22.25 - 0.5\log_{10}h_{UAV}\right) \times \log_{10}d_{3D} + 20\log_{10}\frac{f_c}{1000}\right) \quad (2)$$

$$\text{Rural} = 20\log_{10}\left(\frac{40\pi\left(\frac{f_c}{1000}\right)}{3}\right) + max\left(\left(23.9 - 1.8\log_{10}hUAV\right), 20\right) \times \log_{10}(d_{3D}) \quad (3)$$

$$PL_{ITU-R} = 10\alpha\log_{10}(d_{3D}) + \beta + 10\gamma\log_{10}\left(\frac{f_c}{1000}\right) \quad (4)$$

$$PL_{dB} = \begin{cases} f'_{COST}(d_{2D} = d_{BK}) + \Delta_{CF}(h_{BS}), & 0 \leq d_{2D} \leq d_{BK}, 0 \leq h_{BS} \leq h_{CF} \\ f'_{COST}(d_{2D}) + \Delta_{CF}(h_{BS}), & d_{BK} < d_{2D} \leq d_{CF}, 0 \leq h_{BS} \leq h_{CF} \end{cases} \quad (5)$$

$$f'_{COST} = a_1 + a_2\log_{10}(f_c) + a_3\log_{10}(h_{BS}) - \Gamma(h_{UAV}) + \left[a_4 + a_5\log_{10}(h_{BS})\right]\log_{10}\left(\frac{d_{2D}}{1000}\right) \quad (6)$$

$$\Gamma(h_{UE}) = \left[1.1\log_{10}(f_c) - 0.7\right]h_{UAV} - 1.56\log_{10}(f_c) + 0.8 \quad (7)$$

$$\Delta_{CF}(h_{BS}) = b(f_c)\log_{10}^2(h_{BS}) \quad (8)$$

$$PL_{UMa}(f_c, d_{3D}, h_{UAV}) = PL_{UMa}^{3GPP}(f_c, d_{3D}) + CF_{UMa}(h_{UAV}) \quad (9)$$

$$PL_{UMa}^{3GPP}(f_c, d_{3D}) = 28 + 22\log_{10}(d_{3D}) + 20\log_{10}\left(\frac{f_c}{1000}\right) \quad (10)$$

$$CF_{UMa}(h_{UAV}) = 1.0005 \times 10^{-4}h_{UAV}^2 - 0.0286h_{UAV} + 10.5169 \quad (11)$$

$$PL_{RMa}(f_c, d_{3D}, d_{2D}, h_{Blg}) = PL_{RMa}^{3GPP}(f_c, d_{3D}, h_{Blg}) + CF_{RMa}(d_{2D}) \quad (12)$$

$$PL_{RMa}^{3GPP}(f_c, d_{3D}, h_{Blg}) = 20\log_{10}\left(\frac{40\pi\frac{f_c}{1000}}{3}d_{3D}\right) + min\left(0.03h_{Blg}^{1.72}, 10\right)\log_{10}(d_{3D}) - min\left(0.044h_{Blg}^{1.72}, 14.77\right) \quad (13)$$

$$CF_{RMa}(d_{2D}) = \begin{cases} 2.8359\log_{10}\left(\frac{1000}{d_{2D}}\right) + 13.2785, & 1 \leq d_{2D} \leq 4km \\ 3.9745\log_{10}\left(\frac{1000}{d_{2D}}\right) + 13.9739, & 4 \leq d_{2D} \leq 10km \end{cases} \quad (14)$$

TABLE 5. The coefficients in matolak model.

Setting		Urban (Cleveland)		Suburban (Palmdale)		Rural (Hilly, Latrobe)	
Band		C-band	L-band	C-band	L-band	C-band	L-band
Log-distance PL Model	$A_0(dB)$	110.4	99.4	116.7	98.2	115.4	96.1
	n	2	1.7	1.5	1.7	1.8	1.8
	$\sigma_X(dB)$	3.2	2.6	2.9	3.1	2.7	3.2
	X_{max}	-	-	-	-	8.6	17.5
	$F(dB)$	2.3	1.8	0	1.1	2.3	2.1
Link Range	$R_{min}(m)$	1700	1600	2600	1300	2400	1300
	$R_{max}(m)$	19000	19000	16900	16900	1300	1300

C. RESEARCH GAP ANALYSIS OF MODELS

In this section, we highlight the uniqueness, crucial requirements, and potential applications of each empirical model. Generally, the UAV empirical models selected for this work are modified versions of terrestrial models. The modification in the terrestrial models has been made based on UAV field test findings. First, the Matolak model is a modified version of the log-distance model with added travelling direction parameters for UAVs to travel towards and away from the transmitter. Secondly, the 3GPP modified model is proposed for UAV applications with added height-dependent parameters in the 3GPP TR 38.901 terrestrial model [65]. The Amorim model is a modified version of the log-distance model with added height-dependent parameters in the model for UAV application. The COST Hata modified model is a modified version of the original COST Hata terrestrial model [66]. The modification has been made by including UAV and ground station height-dependent correction factors in the terrestrial model. At the same time, the ITU-R.P.1411-11 propagation over roof-tops site general model is used in this analysis. This site-general model applies to situations where one of the stations is located above the rooftop, and the other station is located below the rooftop, regardless of their antenna heights.

Since different empirical models are developed based on different frequency settings and considerations, it is challenging to find consensus on a single frequency range among these independent models for AG channel analysis. Therefore, we have considered three main frequencies, namely 925 MHz (low band), 2400 MHz (mid band), and 5000 MHz (high band). The 925 MHz band is selected to observe AG channel behaviour at the lower frequency band. Meanwhile, the 2400 MHz and 5000 MHz frequencies were selected as two different ISM bands. The most relevant empirical models for each of the frequencies are selected and evaluated.

As previously indicated, the 3GPP TR 36.777 model is introduced to facilitate integration into LTE networks. This model encompasses three distinctive scenarios: urban, suburban, and rural, each accompanied by explicit altitude and horizontal distance restrictions. The upper limit for altitude within this model is set at 300 m. In parallel, for urban and suburban contexts, the horizontal span remains under 4000 m, while in rural areas, it is confined to under 10000 m. Simultaneously, the 3GPP modified model constitutes an adaptation of the 3GPP TR 38.901 model. This adjustment incorporates factors such as UAV height-based corrections, average building heights within surrounding environments, and a breakpoint at a horizontal distance of 4000 m. The 3GPP modified model was introduced to characterise channels operating at 919 MHz and 2412 MHz frequencies, the 3GPP modified model accommodates altitudes between 50 m and 150 m. For urban scenarios, the horizontal distance spans from 145 m to 320 m, while rural scenarios extend from 1000 m to 10000 m. For the ITU-R model, there is no designated range for permissible altitude however, the acceptable horizontal distance ranges from 55 m to 1200 m. This model is introduced for urban and suburban settings at frequencies up to 73000 MHz. In contrast, the COST-Hata modified model is tailored to frequencies of 785 MHz and 2160 MHz, featuring a horizontal distance cap of 70000 m and an altitude range from 30 m to 1000 m. Exclusive to rural environments, the Amorim model specified a horizontal distance range of 1000 m to 22000 m, with an altitude ceiling of 120 m. The Matolak model has a horizontal distance breaking point of 1300 m for suburban and rural environments and 1600 m for urban environments, as stated in Table 5. On top of that, this model has proposed for L-band (960 MHz) and C-band (5060 MHz) frequencies with the UAV flying at altitudes higher than 500 m.

The simulation was performed based on the required horizontal distance of 2000 m to 10000 m as well as a lower horizontal distance of 100 m to 1000 m. The purpose of the simulation is to verify the potential horizontal distance that can be supported by the models apart from the one reported by the respective models. The maximum UAV altitude reported by the 3GPP model is 300 m, the Amorim model is 120 m, the 3GPP modified model is 150 m, and the Matolak model is, on average 500 m. The main purpose of varying the altitude is to observe the effect of height on the AG channel. The simulation results reported in this work are based on varying the altitude (50 m, 100 m, and 300 m) while

TABLE 6. Summary of research gap analysis.

Ref.	Empirical PL Model	Scenario	Important factors	Uniqueness	Frequency	Horizontal distance	Gap analysis
[26]	3GPP TR36.777	Urban, suburban, rural	UAV height, link distance, frequency	- Introduced to facilitate integration into LTE networks	800 MHz & 2000-2600 MHz	Urban & Suburban: ≤ 4 km Rural: ≤ 10 km	- Does not support altitude beyond 300 m - Not applicable to frequency more than 2600 MHz
[27]	ITU-R P. 1411-11	Urban, suburban	Link distance, frequency	- Site general model - Do not depend on antenna height	2200-73000 MHz	55 – 1200 m	- Does not support rural environment - Not applicable to frequency lower than 2200 MHz
[28]	COST Hata Modified	Urban, suburban, rural	Horizontal distance, UAV height, frequency	- Modified COST Hata terrestrial model - Added height-dependent correction factor	785 MHz & 2160 MHz	Max 70 km	- Does not support for altitude below 30 m and above 1 km - Suitable for frequencies 785 MHz and 2160 MHz only
[38]	3GPP TR38.901 Modified	Urban, rural	UAV height, link distance, building height, frequency	- Modified TR38.901 model - Introduced height-dependent parameter	919 MHz & 2412 MHz	145 – 320 m & 1 – 10 km	- Not applicable to suburban environment. - Support only altitude ranging from 50 m to 150 m
[39]	Amorim	Rural	UAV height, link distance	- Modified log-distance model - Introduced height-dependent parameter	800 MHz	1 – 22 km	- Does not support urban and suburban environment - The altitude is limited to 120 m
[40]–[42]	Matolak	Urban, suburban, rural/hilly and mountainous	Traveling direction, link distance	- Modified log-distance model - Added traveling direction	L-band: 960 MHz C-band: 5060 MHz	720 m – 46 km	- Not applicable for frequency other than L-band and C-band - Does not support UAV altitude below 500 m

keeping the horizontal distance fixed at 100 m-1000 m and 2000 m - 10000 m.

3GPP TR 36.777, Amorim, Matolak, and 3GPP modified are chosen for analysis at 925 MHz frequency. The frequency covered for these models is in the range from 800 MHz to 960 MHz. With the exception of the Matolak model, which has an altitude higher than 504 m, all the other models have altitudes ranging from 10 m to 300 m. The horizontal distance covered more than 1000 m except for the 3GPP modified model in the urban environment which falls in the range of 145 – 320 m. Hence, these models could be deemed suitable for evaluation at 925 MHz and can be optimised for lower horizontal distances.

For 2400 MHz frequency, 3GPP TR 36.777, 3GPP modified, COST Hata Modified, and ITU-R models are selected as suitable models for analysis. The frequency ranges of the models fall between 2000 - 2600 MHz range. The horizontal distance covered for above 1000 m distance. Therefore, these models have the potential to be considered at 2400 MHz, and horizontal distance can focus on less than 1000 m.

At 5000 MHz frequency, Matolak, 3GPP TR 36.777, and ITU models are the compatible models. The minimum altitude for the Matolak model is 500 m, and the 3GPP TR 36.777 model is 10 m for rural and 22.5 for urban and suburban environment. The considered horizontal distance is from 55 m onwards for the ITU-R model and 720 m onwards for the Matolak models. The potential gaps that can be covered with this model for altitude are 50 m, 100 m, and 300 m, and horizontal distance for less than 1000 m.

In addition, it is worth noting that the number of measurements, the building structure and its materials, the ground structure, and its properties as well as the type of vegetation could create a discrepancy between the models. The analysis of the research gap is summarised in Table 6.

V. ANALYSIS AND DISCUSSION

In this section, we discuss the results obtained from simulation for all the above-mentioned UAV empirical models.

Generally, the models are divided into three main frequencies, which are 925 MHz, 2400 MHz, and 5000 MHz, as explained in section IV-C. In terms of UAV's altitude, we focused on three standard altitudes such as 50 m, 100 m, and 300 m. These altitudes are selected for simulation as most of the empirical models analysed in this work covered the average maximum altitude of 300 m. For the horizontal distance, we divide the analysis into two categories, such as a higher UAV's horizontal distance (2000 m to 10000 m) as an

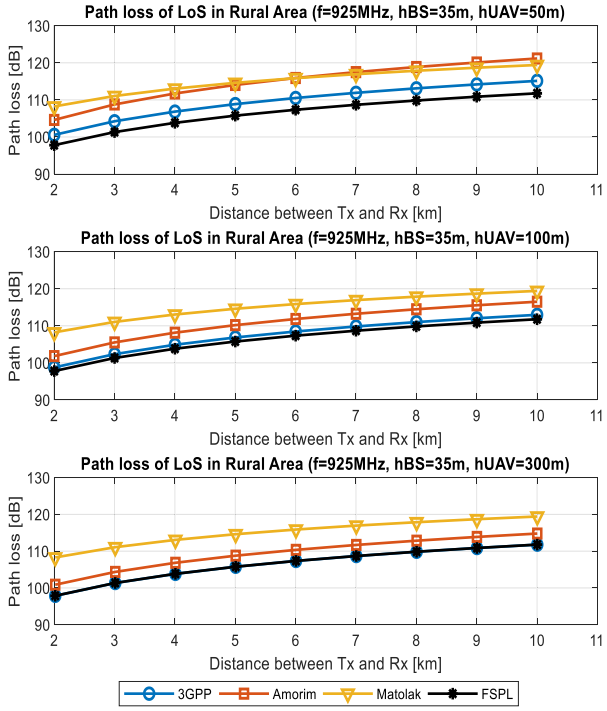

FIGURE 3. 3GPP, Amorim, Matolak, and FSPL models comparison at 925 MHz at heights of UAV 50 m, 100 m, and 300 m for the rural environment (actual range).

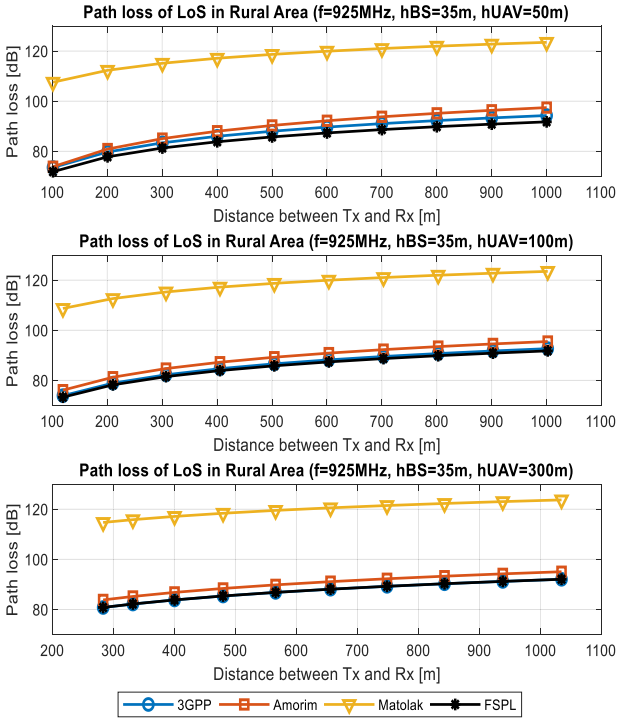

FIGURE 4. 3GPP, Amorim, Matolak, and FSPL models comparison at 925 MHz at heights of UAV 50 m, 100 m, and 300 m for the rural environment (exploited range).

actual range and a lower UAV's horizontal distance (100 m to 1000 m) as an exploited range of models. Lower horizontal distances were selected as the exploitation range for simulation because most of the empirical models considered in this work covered a longer distance of more than 2000 m. The purpose of this analysis is to verify the horizontal distance effect on path loss of AG channels in urban, suburban, and rural environments.

For 925 MHz, the 3GPP, Amorim, and Matolak models are used for the rural environment. Only these models are considered as they have performed UAV AG measurement at low frequency, as stated in Table 1. Figure 3 shows the path loss simulation following the actual requirements of the models. It was observed that the 3GPP model becomes 100 % compatible with FSPL at a height of 300 m. The path loss of the Amorim model reduces as the altitude increases. The path loss of the Matolak model remains the same as 120 dB at 50 m, 100 m, and 300 m UAV altitudes. The 3GPP model is a modified version of FSPL. Thus, the prediction of both models is the same when UAVs fly at an altitude of 300 m onwards. According to the Amorim model, the altitude value is compared between UAV altitude and FSPL altitude. Thus, the model's path loss gets lesser as UAV altitude increases. This is proven in [39], where the path loss exponent decays with the increase in UAV height, resulting in a noticeable discrepancy in the path loss attenuation at a larger distance. For instance, over longer path distances that are close to 10000 m, the signal attenuation is 20 dB higher on the ground compared to the measurements taken at 120 m height.

Since the applicable horizontal distance for each model is different, two results which are based on the actual horizontal distance range stated by the model (actual range) and another horizontal distance that is not within the range of the model (exploited range) were analysed for comparison purpose in this work. Figure 4 shows the result simulated using the exploited range for lower UAV's horizontal distance as stated by the model. The path loss of the Matolak model remains the same at all three heights. While the 3GPP model becomes 100 % compatible with the FSPL model starting at a 100 m altitude. The Amorim model closely follows the 3GPP and FSPL model at a lower UAV's horizontal distance. Overall, at 925 MHz frequency, the path loss is lower when it operates at a lower UAV's horizontal distance of less than 1000 m in a rural environment. The 3GPP model can be selected as the most optimistic empirical model for UAVs operating at 925 MHz in rural environments, followed by the Amorim and Matolak models.

For UAVs operating at 925 MHz frequency in an urban environment, Matolak, 3GPP, and 3GPP modified models are compared as they fulfilled all the requirements for the simulation. Similar to the rural environment, the simulation was performed at higher and lower horizontal distances of UAVs are shown in Figures 5 and 6, respectively. For the actual range, the Matolak and 3GPP models follow closely with the FSPL model for all three UAV altitudes. The path loss also remains constant throughout three UAV altitudes as these two models do not depend on the UAV's altitude. In this respect, the 3GPP modified model displays higher path loss

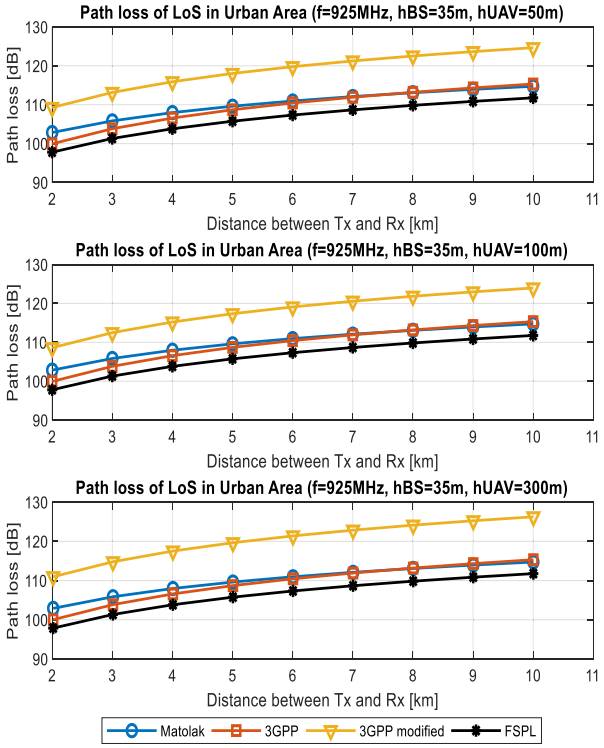

FIGURE 5. Matolak, 3GPP, and 3GPP modified models comparison at 925 MHz at heights of UAV 50 m, 100 m, and 300 m for the urban environment (actual range).

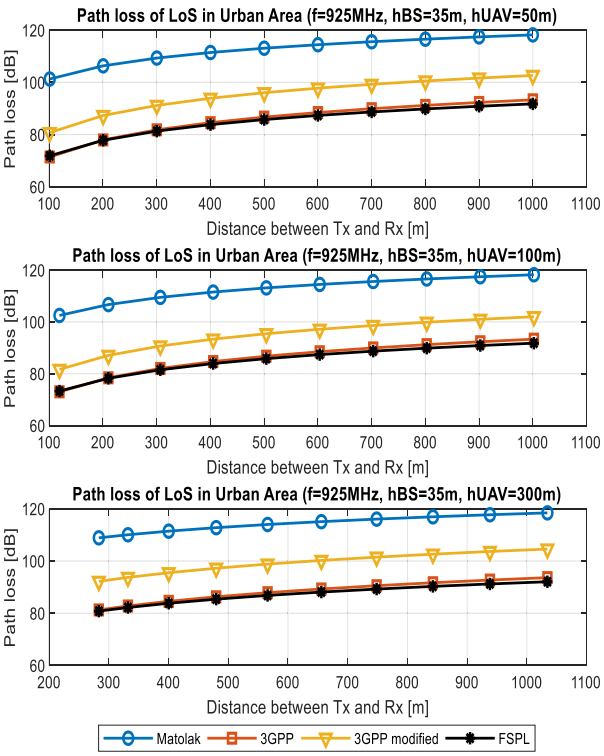

FIGURE 6. Matolak, 3GPP, and 3GPP modified models comparison at 925 MHz at heights of UAV 50 m, 100 m, and 300 m for the urban environment (exploited range).

compared to other models in an urban environment. However, for the exploited range at a lower horizontal distance of

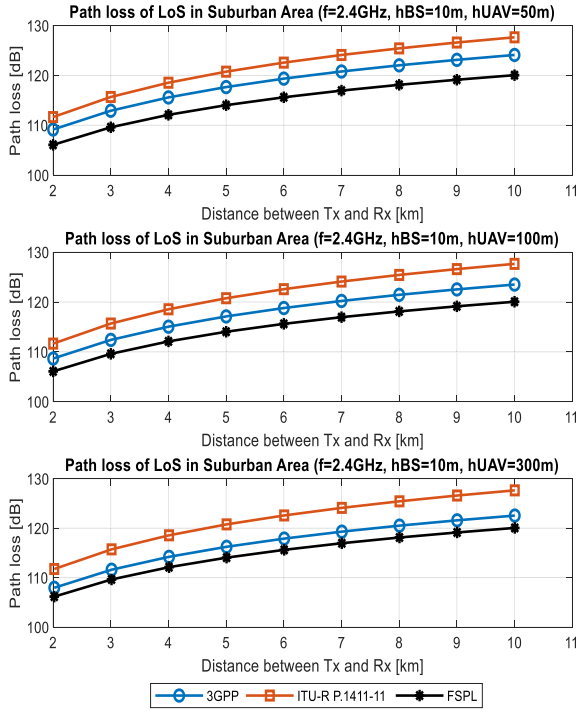

FIGURE 7. 3GPP, ITU-R, and FSPL models comparison at 2.4 GHz at heights of UAV 50 m, 100 m, and 300 m for the suburban environment (actual range).

UAV as shown in Figure 6, both 3GPP and 3GPP modified models follow closely with FSPL models for all three UAV altitudes, while the Matolak model achieved the highest path loss among them. In general, at 925 MHz, the path loss value remains consistent for higher UAV horizontal distances in the urban environment. In the context of UAV applications operating at 925 MHz within the urban environment, the 3GPP model emerges as the most optimistic empirical model for shorter horizontal distance, succeeded by the 3GPP modified and Matolak models. Nevertheless, for higher horizontal distances, the 3GPP model takes precedence as the most optimistic, closely followed by the Matolak and 3GPP modified models.

On the other hand, UAV application at 2400 MHz for suburban environments, the 3GPP and ITU-R models are compared. The simulated results show that, for higher horizontal distances at 10000 m, the path loss for FSPL, 3GPP, and ITU-R models remains consistent at 120 dB, 122 dB, and 128 dB, respectively, as shown in Figure 7 for all altitudes, while for lower horizontal distance, path loss by ITU model is higher compared to 3GPP model, which closely resembles the FSPL model in Figure 8. In general, it can be observed that the higher horizontal distance of UAVs achieves higher path loss than the lower one. The 3GPP and ITU-R models are deemed compatible with UAV applications at 2400 MHz in a suburban environment. In terms of the model selection at 2400 MHz, 3GPP is more optimistic and ITU-R is pessimistic at both lower and higher horizontal distances in a suburban environment.

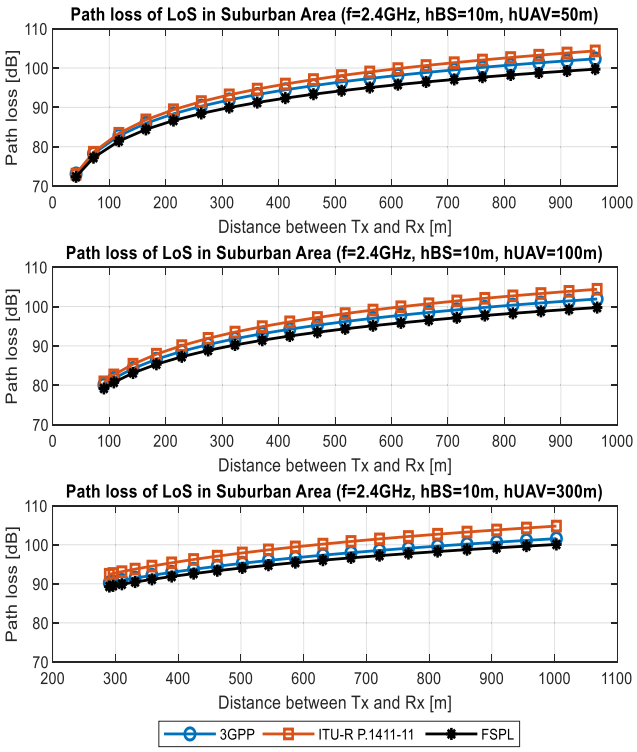

FIGURE 8. 3GPP, ITU-R, and FSPL models comparison at 2.4 GHz at heights of UAV 50 m, 100 m, and 300 m for the suburban environment (exploited range).

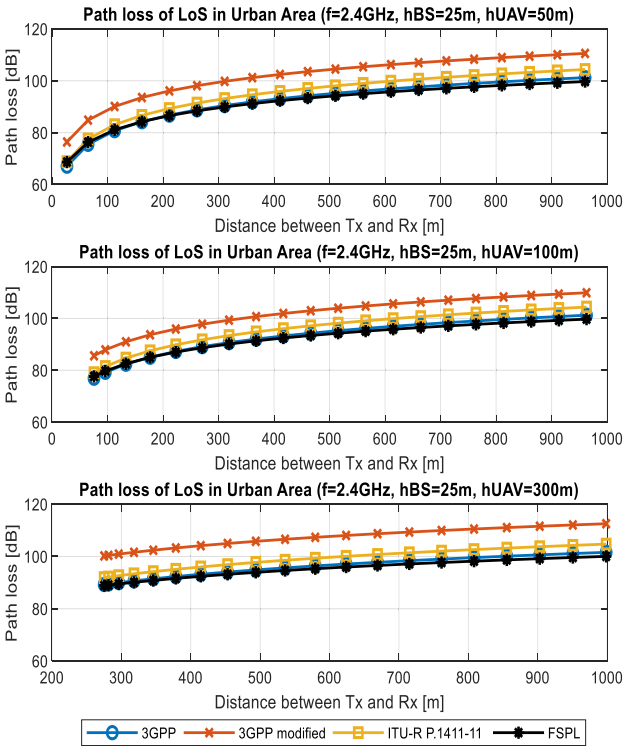

FIGURE 10. 3GPP, 3GPP modified, and ITU-R models comparison at 2.4 GHz at heights of UAV 50 m, 100 m, and 300 m for the urban environment (exploited range).

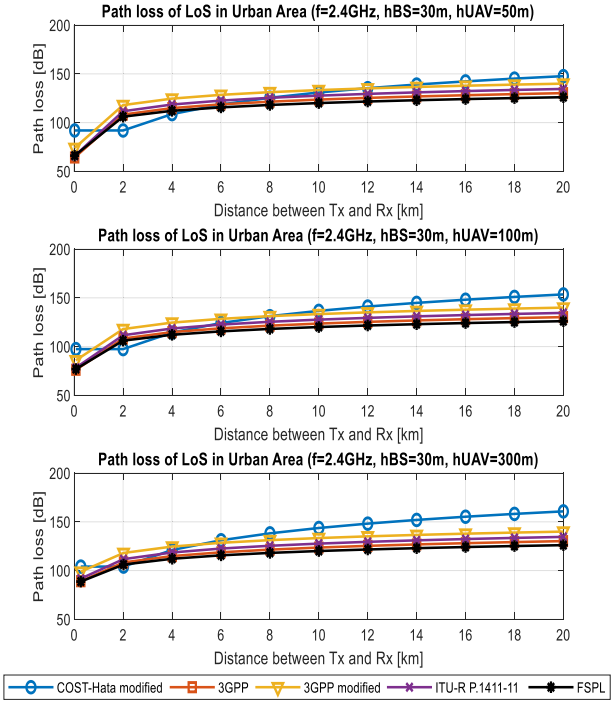

FIGURE 9. COST Hata modified, 3GPP, 3GPP modified, and ITU-R models comparison at 2.4 GHz at heights of UAV 50 m, 100 m, and 300 m for the urban environment (actual range).

Figures 9 and 10 show the simulation results for UAV application at 2400 MHz for the urban environment at higher and lower UAV horizontal distances, respectively. COST Hata modified, 3GPP, 3GPP modified, and ITU-R models are compared. Since the COST Hata modified model result is not reliable for lower UAV's horizontal distance due to the horizontal distance requirement must be greater than 2000 m, hence the model is omitted in Figure 10. The path loss of 3GPP, 3GPP modified, and ITU models remains consistent at 50 m to 300 m altitude, while the COST Hata modified model's path loss increases about 1 dB from 50 m to 300 m altitude. For lower UAV's horizontal distance, the 3GPP, 3GPP modified, and the ITU model path loss remains the same in all three altitudes. Based on the findings, the advisable choice for an urban scenario at 2400 MHz is the 3GPP model. This selection is justified by the model's close alignment with the FSPL model, as well as its proximity to the ITU-R and 3GPP modified models, spanning both shorter and longer horizontal distances. Notably, the COST-Hata modified model demonstrates comparatively lower pessimism at 2400 MHz in an urban environment.

When the frequency increased to 5000 MHz for the urban environment at 2700 m horizontal distance, both the Matolak and 3GPP models path loss remained constant at 116.5 dB and 117 dB, respectively for all three altitudes, while the ITU-R model remained constant at 121 dB as shown in Figure 11. The path loss of all three models shows an increasing trend from 1700 m to 2700 m distance. It seems that the Matolak model appeared closest to the FSPL model and most optimistic, while the ITU-R model is the most pessimistic for

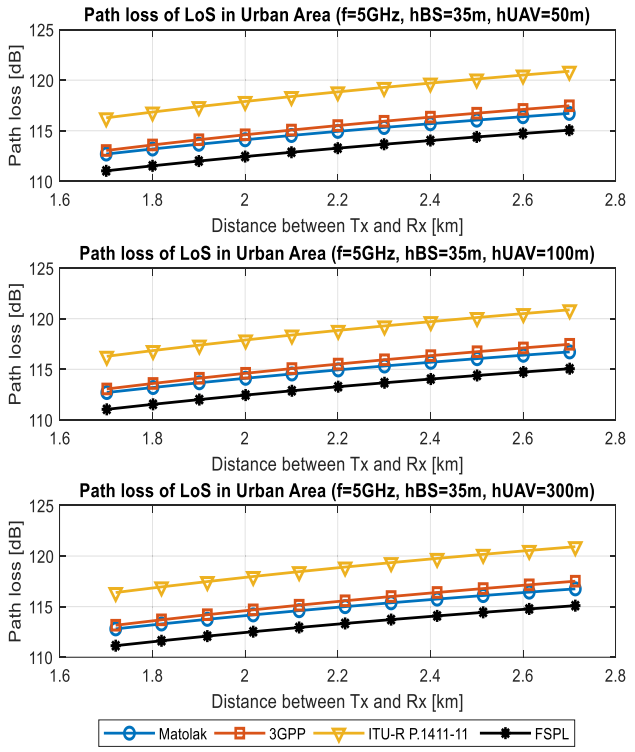

FIGURE 11. Matolak, 3GPP, ITU-R, and FSPL models comparison at 5 GHz at heights of UAV 50 m,100 m, and 300 m for the urban environment (actual range).

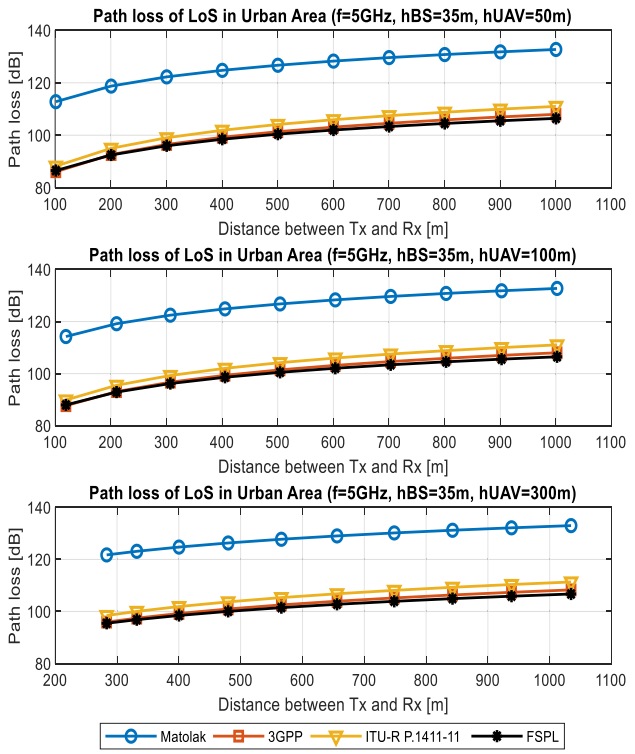

FIGURE 12. Matolak, 3GPP, ITU-R, and FSPL models comparison at 5 GHz at heights of UAV 50 m,100 m, and 300 m for the urban environment (exploited range).

the actual range. On the other hand, as shown in Figure 12, when all the models are investigated for the exploited range, the Matolak model achieves the highest path loss than the ITU-R model, followed by the 3GPP model. For this scenario, the 3GPP model is the most optimistic, while the Matolak model is the most pessimistic.

For lower UAV horizontal distance applications, the 3GPP model is the suitable model for urban, suburban, and rural environments at 925 MHz, 2400 MHz, and 5000 MHz. It is also a model for UAV altitudes from 50 m to 300 m. The Matolak model is the least suitable model for lower UAV's horizontal distance at 925 MHz and 5000 MHz. At 2400 MHz, the ITU-R model and 3GPP modified model are the least suitable models for suburban and urban environments, respectively.

For higher UAV horizontal distance applications, the Matolak model is the most suitable model for urban environments at 925 MHz and 5000 MHz. The 3GPP model is also suitable for the rural environment at 925 MHz. For 2400 MHz, the 3GPP model is the most suitable model for urban and suburban environments. In the least suitable category, we have a 3GPP modified model for the urban environment at 925 MHz and the ITU-R model for the urban, suburban, and rural environment at 5000 MHz.

VI. CONCLUSION AND FUTURE WORK

In this work, a list of empirical models for UAV aerial links is gathered and compared based on the models' features and the parameter ranges considered in the channel measurement campaign. These empirical models include the 3GPP model, ITU-R P.1411-11 model, COST Hata modified model, 3GPP modified model, Amorim model, and Matalok model. Detailed analysis and discussion have been conducted based on the key parameters that affect the path loss. The research gaps among these empirical models are identified to motivate potential measurement campaigns in the future. Eventually, quantitative insights on the path loss values generated from different empirical models and comparisons of different path loss models over different parameters and settings are provided accordingly. Such insights could further improve our understanding on the discrepancies and limitations of the existing empirical models and motivate measurement campaigns in the future.

In forthcoming research, an investigation could be conducted into the additional path loss arising from tropical vegetation, weather conditions, atmospheric absorption, as well as obstacles and terrain. Emphasis shall also be placed on exploring measurements to identify correction factors, thereby enhancing the predictive capabilities of models in subsequent research efforts. The improvement of predictive models for UAV communication scenarios in real-world settings will be a key focus of future work. Nevertheless, a comprehensive understanding of wireless channel behaviour necessitates a deeper exploration of the intricate dynamics of small-scale fading induced by multipath propagation. In scenarios where multiple signal paths interact, refining the accuracy of channel models will involve investigating the complex interplay of these fading events.

REFERENCES

[1] C. Zhang, W. Zhang, W. Wang, L. Yang, and W. Zhang, "Research challenges and opportunities of UAV millimeter-wave communications," *IEEE Wireless Commun.*, vol. 26, no. 1, pp. 58–62, Feb. 2019.

[2] W. K. New and C. Y. Leow, "Unmanned aerial vehicle (UAV) in future communication system," in *Proc. 26th IEEE Asia–Pacific Conf. Commun. (APCC)*, Oct. 2021, pp. 217–222.

[3] Q. Zhu and J. Zheng, "Coverage recovery analysis of UAV base station networks," in *Proc. IEEE Global Commun. Conf.*, Dec. 2020, pp. 1–6.

[4] A. K. Patel and R. D. Joshi, "Area coverage analysis of low altitude UAV bases station using statistical channel model," in *Proc. Int. Conf. Signal Inf. Process. (IConSIP)*, Aug. 2022, pp. 1–6.

[5] S. A. Al-Ahmed, M. Z. Shakir, and S. A. R. Zaidi, "Optimal 3D UAV base station placement by considering autonomous coverage hole detection, wireless backhaul and user demand," *J. Commun. Netw.*, vol. 22, no. 6, pp. 467–475, Dec. 2020.

[6] S. A. H. Mohsan, N. Q. H. Othman, Y. Li, M. H. Alsharif, and M. A. Khan, "Unmanned aerial vehicles (UAVs): Practical aspects, applications, open challenges, security issues, and future trends," *Intell. Service Robot.*, vol. 16, pp. 109–137, Jan. 2023.

[7] J. Zhao, F. Gao, G. Ding, T. Zhang, W. Jia, and A. Nallanathan, "Integrating communications and control for UAV systems: Opportunities and challenges," *IEEE Access*, vol. 6, pp. 67519–67527, 2018.

[8] Y. Zeng, R. Zhang, and T. J. Lim, "Wireless communications with unmanned aerial vehicles: Opportunities and challenges," *IEEE Commun. Mag.*, vol. 54, no. 5, pp. 36–42, May 2016.

[9] D. Rakesh, N. A. Kumar, M. Sivaguru, K. V. R. Keerthivaasan, B. R. Janaki, and R. Raffik, "Role of UAVs in innovating agriculture with future applications: A review," in *Proc. Int. Conf. Advancements Electr., Electron., Commun., Comput. Autom. (ICAECA)*, Oct. 2021, pp. 1–6.

[10] S. Moradi, A. Bokani, and J. Hassan, "UAV-based smart agriculture: A review of UAV sensing and applications," in *Proc. 32nd Int. Telecommun. Netw. Appl. Conf.*, 2022, pp. 181–184.

[11] S. Hayat, E. Yanmaz, and R. Muzaffar, "Survey on unmanned aerial vehicle networks for civil applications: A communications viewpoint," *IEEE Commun. Surveys Tuts.*, vol. 18, no. 4, pp. 2624–2661, 4th Quart., 2016.

[12] H. Shakhatreh, A. H. Sawalmeh, A. Al-Fuqaha, Z. Dou, E. Almaita, I. Khalil, N. S. Othman, A. Khreishah, and M. Guizani, "Unmanned aerial vehicles (UAVs): A survey on civil applications and key research challenges," *IEEE Access*, vol. 7, pp. 48572–48634, 2019.

[13] S. A. H. Mohsan, M. A. Khan, F. Noor, I. Ullah, and M. H. Alsharif, "Towards the unmanned aerial vehicles (UAVs): A comprehensive review," *Drones*, vol. 6, no. 6, p. 147, Jun. 2022.

[14] W. K. New, C. Y. Leow, K. Navaie, and Z. Ding, "Robust non-orthogonal multiple access for aerial and ground users," *IEEE Trans. Wireless Commun.*, vol. 19, no. 7, pp. 4793–4805, Jul. 2020.

[15] P. S. Bithas, V. Nikolaidis, A. G. Kanatas, and G. K. Karagiannidis, "UAV-to-ground communications: Channel modeling and UAV selection," *IEEE Trans. Commun.*, vol. 68, no. 8, pp. 5135–5144, Aug. 2020.

[16] D. Tse and P. Viswanath, *Fundamentals of Wireless Communications*. USA: Cambridge Univ. Press, 2005.

[17] T. S. Rappaport, *Wireless Communications: Principles and Practice*. Upper Saddle River, NJ, USA: Prentice-Hall, 2002.

[18] Z. Yun and M. F. Iskander, "Ray tracing for radio propagation modeling: Principles and applications," *IEEE Access*, vol. 3, pp. 1089–1100, 2015.

[19] P. Kumar, P. Singh, S. Darshi, and S. Shailendra, "Analysis of drone assisted network coded cooperation for next generation wireless network," *IEEE Trans. Mobile Comput.*, vol. 20, no. 1, pp. 93–103, Jan. 2021.

[20] P. Kumar and S. Majhi, "UAV-assisted network coded cooperation by using height-dependency shaping parameters in Nakagami-*m* faded channel," *IEEE Access*, vol. 12, pp. 11688–11699, 2024.

[21] P. Kumar, S. Bhattacharyya, S. Darshi, S. Majhi, A. A. Almohammedi, and S. Shailendra, "Outage analysis using probabilistic channel model for drone assisted multi-user coded cooperation system," *IEEE Trans. Veh. Technol.*, vol. 72, no. 8, pp. 10273–10285, Aug. 2023.

[22] J. Won, D.-Y. Kim, Y.-I. Park, and J.-W. Lee, "A survey on UAV placement and trajectory optimization in communication networks: From the perspective of air-to-ground channel models," *ICT Exp.*, vol. 9, no. 3, pp. 385–397, Jun. 2023.

[23] S. Zhang and R. Zhang, "Radio map-based 3D path planning for cellular-connected UAV," *IEEE Trans. Wireless Commun.*, vol. 20, no. 3, pp. 1975–1989, Mar. 2021.

[24] J. Chen and D. Gesbert, "Efficient local map search algorithms for the placement of flying relays," *IEEE Trans. Wireless Commun.*, vol. 19, no. 2, pp. 1305–1319, Feb. 2020.

[25] D.-Y. Kim, W. Saad, and J.-W. Lee, "On the use of high-rise topographic features for optimal aerial base station placement," *IEEE Trans. Wireless Commun.*, vol. 22, no. 3, pp. 1868–1884, Mar. 2023.

[26] *Study on Enhanced LTE Support for Aerial Vehicles*, document TR 36.777, 3GPP, 2017.

[27] *Propagation Data and Prediction Methods for the Planning of Short-Range Outdoor Radiocommunication Systems and Radio Local Area Networks in the Frequency Range 300 MHz to 100 GHz*, document ITU-R 11-1411, 2021, pp. 1–54.

[28] R. Zhang, Q. Guo, D. Zhai, D. Zhou, X. Du, and M. Guizani, "Channel measurement and resource allocation scheme for dual-band airborne access networks," *IEEE Access*, vol. 7, pp. 80870–80883, 2019.

[29] Y. Li, N. Li, and C. Han, "Ray-tracing simulation and hybrid channel modeling for low-terahertz UAV communications," in *Proc. IEEE Int. Conf. Commun.*, Jun. 2021, pp. 1–6.

[30] X. Cai, A. Gonzalez-Plaza, D. Alonso, L. Zhang, C. B. Rodríguez, A. P. Yuste, and X. Yin, "Low altitude UAV propagation channel modelling," in *Proc. 11th Eur. Conf. Antennas Propag. (EUCAP)*, Mar. 2017, pp. 1443–1447.

[31] W. Khawaja, I. Guvenc, and D. Matolak, "UWB channel sounding and modeling for UAV air-to-ground propagation channels," in *Proc. IEEE Global Commun. Conf. (GLOBECOM)*, Dec. 2016, pp. 1–7.

[32] Z. Cui, C. Briso-Rodríguez, K. Guan, Z. Zhong, and F. Quitin, "Multi-frequency air-to-ground channel measurements and analysis for UAV communication systems," *IEEE Access*, vol. 8, pp. 110565–110574, 2020.

[33] J. Allred, A. B. Hasan, S. Panichsakul, W. Pisano, P. Gray, J. Huang, R. Han, D. Lawrence, and K. Mohseni, "SensorFlock: An airborne wireless sensor network of micro-air vehicles," in *Proc. 5th ACM Conf. Embedded Networked Sensor Syst.*, 2007, pp. 117–129.

[34] A. Shaw and K. Mohseni, "A fluid dynamic based coordination of a wireless sensor network of unmanned aerial vehicles: 3-D simulation and wireless communication characterization," *IEEE Sensors J.*, vol. 11, no. 3, pp. 722–736, Mar. 2011.

[35] N. Ahmed, S. S. Kanhere, and S. Jha, "On the importance of link characterization for aerial wireless sensor networks," *IEEE Commun. Mag.*, vol. 54, no. 5, pp. 52–57, May 2016.

[36] E. Yanmaz, S. Hayat, J. Scherer, and C. Bettstetter, "Experimental performance analysis of two-hop aerial 802.11 networks," in *Proc. IEEE Wireless Commun. Netw. Conf. (WCNC)*, Apr. 2014, pp. 3118–3123.

[37] E. Yanmaz, R. Kuschnig, and C. Bettstetter, "Achieving air-ground communications in 802.11 networks with three-dimensional aerial mobility," in *Proc. IEEE INFOCOM*, Apr. 2013, pp. 120–124.

[38] K. Wang, R. Zhang, L. Wu, Z. Zhong, L. He, J. Liu, and X. Pang, "Path loss measurement and modeling for low-altitude UAV access channels," in *Proc. IEEE 86th Veh. Technol. Conf. (VTC-Fall)*, Sep. 2017, pp. 1–5.

[39] R. Amorim, H. Nguyen, P. Mogensen, I. Z. Kovács, J. Wigard, and T. B. Sørensen, "Radio channel modeling for UAV communication over cellular networks," *IEEE Wireless Commun. Lett.*, vol. 6, no. 4, pp. 514–517, Aug. 2017.

[40] D. W. Matolak and R. Sun, "Air–ground channel characterization for unmanned aircraft systems—Part I: Methods, measurements, and models for over-water settings," *IEEE Trans. Veh. Technol.*, vol. 66, no. 1, pp. 26–44, Jan. 2017.

[41] R. Sun and D. W. Matolak, "Air–ground channel characterization for unmanned aircraft systems—Part II: Hilly and mountainous settings," *IEEE Trans. Veh. Technol.*, vol. 66, no. 3, pp. 1913–1925, Mar. 2017.

[42] D. W. Matolak and R. Sun, "Air-ground channel characterization for unmanned aircraft systems—Part III: The suburban and near-urban environments," *IEEE Trans. Veh. Technol.*, vol. 66, no. 8, pp. 6607–6618, Aug. 2017.

[43] A. A. Khuwaja, Y. Chen, N. Zhao, M.-S. Alouini, and P. Dobbins, "A survey of channel modeling for UAV communications," *IEEE Commun. Surveys Tuts.*, vol. 20, no. 4, pp. 2804–2821, 4th Quart., 2018.

[44] W. Khawaja, I. Guvenc, D. W. Matolak, U.-C. Fiebig, and N. Schneckenburger, "A survey of air-to-ground propagation channel modeling for unmanned aerial vehicles," *IEEE Commun. Surveys Tuts.*, vol. 21, no. 3, pp. 2361–2391, 3rd Quart., 2019.

[45] C. Yan, L. Fu, J. Zhang, and J. Wang, "A comprehensive survey on UAV communication channel modeling," *IEEE Access*, vol. 7, pp. 107769–107792, 2019.
[46] L. Gupta, R. Jain, and G. Vaszkun, "Survey of important issues in UAV communication networks," *IEEE Commun. Surveys Tuts.*, vol. 18, no. 2, pp. 1123–1152, 2nd Quart., 2016.
[47] M. Mozaffari, W. Saad, M. Bennis, Y.-H. Nam, and M. Debbah, "A tutorial on UAVs for wireless networks: Applications, challenges, and open problems," *IEEE Commun. Surveys Tuts.*, vol. 21, no. 3, pp. 2334–2360, 3rd Quart., 2019.
[48] A. Al-Hourani, S. Kandeepan, and A. Jamalipour, "Modeling air-to-ground path loss for low altitude platforms in urban environments," in *Proc. IEEE Global Commun. Conf.*, Dec. 2014, pp. 2898–2904.
[49] L. Zhang, H. Zhao, S. Hou, Z. Zhao, H. Xu, X. Wu, Q. Wu, and R. Zhang, "A survey on 5G millimeter wave communications for UAV-assisted wireless networks," *IEEE Access*, vol. 7, pp. 117460–117504, 2019.
[50] V. Mayor, R. Estepa, and A. Estepa, "QoS-aware multilayer UAV deployment to provide VoWiFi service over 5G networks," *Wireless Commun. Mobile Comput.*, vol. 2022, pp. 1–13, Jan. 2022.
[51] G. Geraci, A. Garcia-Rodriguez, L. Galati Giordano, D. López-Pérez, and E. Björnson, "Understanding UAV cellular communications: From existing networks to massive MIMO," *IEEE Access*, vol. 6, pp. 67853–67865, 2018.
[52] B. Van Der Bergh, A. Chiumento, and S. Pollin, "LTE in the sky: Trading off propagation benefits with interference costs for aerial nodes," *IEEE Commun. Mag.*, vol. 54, no. 5, pp. 44–50, May 2016.
[53] R. Essaadali and A. Kouki, "A new simple unmanned aerial vehicle Doppler effect RF reducing technique," in *Proc. IEEE Mil. Commun. Conf.*, Nov. 2016, pp. 1179–1183.
[54] M. Ibrahim and H. Arslan, "Air-ground Doppler-delay spread spectrum for dense scattering environments," in *Proc. IEEE Mil. Commun. Conf.*, Oct. 2015, pp. 1661–1666.
[55] A. Al-Hourani, S. Chandrasekharan, S. Kandeepan, and A. Jamalipour, "Aerial platforms for public safety networks and performance optimization," in *Wireless Public Safety Networks 3*. U.K.: Elsevier, 2017, pp. 133–153.
[56] Y. S. Meng and Y. H. Lee, "Measurements and characterizations of air-to-ground channel over sea surface at C-band with low airborne altitudes," *IEEE Trans. Veh. Technol.*, vol. 60, no. 4, pp. 1943–1948, May 2011.
[57] J. Luomala and I. Hakala, "Effects of temperature and humidity on radio signal strength in outdoor wireless sensor networks," in *Proc. Federated Conf. Comput. Sci. Inf. Syst. (FedCSIS)*, Sep. 2015, pp. 1247–1255.
[58] D. M. Mielke, N. Schneckenburger, U.-C. Fiebig, M. Walter, and M. A. Bellido-Manganell, "Analysis of the dominant signal component of the air-ground channel based on measurement data at C-band," *IEEE Trans. Veh. Technol.*, vol. 70, no. 4, pp. 2955–2968, Apr. 2021.
[59] Y. S. Meng and Y. H. Lee, "Study of shadowing effect by aircraft maneuvering for air-to-ground communication," *AEU-Int. J. Electron. Commun.*, vol. 66, no. 1, pp. 7–11, Jan. 2012.
[60] W. Khawaja, O. Ozdemir, and I. Guvenc, "UAV air-to-ground channel characterization for mmWave systems," in *Proc. IEEE 86th Veh. Technol. Conf. (VTC-Fall)*, Sep. 2017, pp. 1–5.
[61] W. Khawaja, O. Ozdemir, F. Erden, I. Guvenc, and D. W. Matolak, "UWB air-to-ground propagation channel measurements and modeling using UAVs," in *Proc. IEEE Aerosp. Conf.*, Mar. 2019, pp. 1–10.
[62] V. Semkin, E. M. Vitucci, F. Fuschini, M. Barbiroli, V. Degli-Esposti, and C. Oestges, "Characterizing the UAV-to-machine UWB radio channel in smart factories," *IEEE Access*, vol. 9, pp. 76542–76550, 2021.
[63] J. Rodríguez-Piñeiro, T. Domínguez-Bolaño, X. Cai, Z. Huang, and X. Yin, "Air-to-ground channel characterization for low-height UAVs in realistic network deployments," *IEEE Trans. Antennas Propag.*, vol. 69, no. 2, pp. 992–1006, Feb. 2021.
[64] N. Blaunstein and C. Christodoulou, *Radio Propagation and Adaptive Antennas for Wireless Communication Networks: Terrestrial, Atmospheric and Ionosphere*. Hoboken, NJ, USA: Wiley, 2014.
[65] *Study on Channel Model for Frequencies From 0.5 to 100 GHz*, document TR 38.901, 3GPP, 2017.
[66] *Urban Transmission Loss Models for Mobile Radio in the 900 and 1,800 MHz Bands (Revision 2)*, COST 231, The Hague, The Netherlands, 1991.

SHI JIE SEAH (Graduate Student Member, IEEE) was born in Kedah, Malaysia, in 1994. She received the bachelor's degree in electronic engineering majoring in communication and the M.Eng. degree in electrical engineering from Universiti Tun Hussein Onn Malaysia, in 2018 and 2021, respectively, where she is currently pursuing the Ph.D. degree in electrical engineering. Her current research interests include wireless propagation and unmanned aerial vehicle (UAV) communication.

CHEE YEN (BRUCE) LEOW (Senior Member, IEEE) received the B.Eng. degree in computer engineering from Universiti Teknologi Malaysia (UTM), in June 2007, and the Ph.D. degree in wireless communications from Imperial College London, in September 2011.

He is currently an Associate Professor with the Faculty of Electrical Engineering, and a Research Fellow with the Wireless Communication Centre, UTM. He is also a Secretary with the IMT and Future Networks Working Group under the Malaysian Technical Standards Forum Berhad to accelerate the adoption of 5G IMT-2020 in Malaysia. In addition, he regularly conducts short courses on 5G and IoT for the telecommunication industry. His current research interests include non-orthogonal multiple access, drone communication, intelligent surfaces, advanced MIMO, millimeter wave communication, prototype development using software-defined radio for beyond 5G, and the Internet of Things applications.

Dr. Leow's IEEE papers won the IEEE Malaysia Comsoc/VTS Joint Chapter's Best Paper Awards, in 2016, 2017, and 2021, and the IEEE Malaysia AP/MTT/EMC Joint Chapter's Best Paper Award, in 2017, 2018, and 2021. He is a registered Chartered Engineer (CEng) of the Engineering Council, U.K.; and a Professional Technologist of the Malaysia Board of Technologists. He is among the pioneers of 5G initiatives in Malaysia to promote 5G Research and Development collaboration between industry and academia.

RENUKA NALINGGAM received the bachelor degree in electrical and electronics engineering from Universiti Tenaga Nasional, in 2005, and the master's and Ph.D degrees in electrical and communication engineering in the field of radio frequency and wave propagation from Universiti Sains Malaysia, in 2011 and 2018, respectively.

From 2011 to 2012, she was a Lecturer with the Asian Institute of Medical, Science and Technology University. From 2016 to 2020, she was a Lecturer with Southern University College, Skudai, Johor. From 2020 to 2022, she was a Post-Doctoral Research Fellow with the Wireless Communication Centre, Universiti Teknologi Malaysia. Her main research interests include machine-to-machine communication, radio-frequency identification, and wireless sensor networks.

WEE KIAT NEW (Member, IEEE) received the B.I.T. degree in data communications and networking from Multimedia University, the M.Eng.Sc. degree in electrical engineering from the University of Malaya, and the Ph.D. degree in electrical engineering from Universiti Teknologi Malaysia. He was a Visiting Researcher with Lancaster University and the University of Cyprus. He is currently a Research Fellow with the Department of Electronic and Electrical Engineering, University College London, U.K. His research interests include information theory, optimization, stochastic processes, and machine learning, and their applications in emerging areas of communications. He was a recipient of the 2021 IEEE Malaysia Comsoc/VTS Best Paper Award, the 2022 IEEE Malaysia AP/MTT/EMC Best Paper Award, the 2021 IEEE Malaysia AP/MTT/EMC Best Paper Award, and the 2020 IEEE Malaysia AP/MTT/EMC Best Paper Award. He served as the TPC Co-Chair for the 2024 ICC Workshop on Fluid Antenna Systems for 6G.

ROZANA ALAM received the B.Sc. degree in information and communication engineering from Bangladesh University of Professionals, in 2019, and the M.Eng. degree in electronic and telecommunication from Universiti Teknologi Malaysia, in 2021, where she is currently pursuing the Ph.D. degree with the School of Electrical Engineering. Her research interests include UAV communication, non-orthogonal multiple access (NOMA), intelligent reflecting surface (IRS), mm-wave communication, channel modeling, and antenna and propagation theory.

SIAT LING JONG was born in Malaysia, in 1982. She received the bachelor's degree in electrical engineering from Universiti Tun Hussein Onn Malaysia, in 2007, and the master's and Ph.D. degrees in electrical and communication engineering in the field of radio wave propagation for satellite communication systems from Universiti Teknologi Malaysia, in 2009 and 2015, respectively.

In 2007, she joined Universiti Tun Hussein Onn Malaysia as an Assistant Lecturer. In 2012 and 2013, she obtained a research attachment grant at Politecnico di Milano, Milan, Italy, to do her research on rain effects and fade dynamics on satellite communication links. Since 2015, she has been a Lecturer of electronic communications with Universiti Tun Hussein Onn Malaysia. She has been involved in the experimental activity of a Ka-band propagation measurement campaign in close collaboration with the European Space Agency (ESA); Joanneum Research, Austria; and Universiti Teknologi Malaysia. She has authored and co-authored several international journals and conferences. Her research interests include rain attenuation, radio wave propagation for satellite communication systems and atmospheric science, statistical modeling, unmanned aerial vehicle (UAV) communication, and the IoT.

Dr. Jong is a Professional Technologist and a member of the Board of Engineers Malaysia (BEM) and the Institution of Engineering and Technology (IET). In 2014, she obtained the Young Scientist Award at the URSI General Assembly and Scientific Symposium. She served as a Reviewer for IEEE Access, IEEE Transactions of Antennas and Propagation, and *IET Microwaves and Antennas*.

HONG YIN LAM received the M.Eng. and Ph.D. degrees in electrical engineering from the University of Technology Malaysia (UTM), in 2009 and 2013, respectively.

In 2014, he was a Postdoctoral Fellow with UTM. Since 2015, he has been with the Department of Electrical Engineering Technology, Faculty of Engineering Technology, Universiti Tun Hussein Onn Malaysia, where he is currently the Head of the Department. He has been involved in several propagation projects, including the project commissioned to the research group by the European Space Agency (ESA). He has authored several contributions to international conferences and scientific journals. His research activities have been related to E.M. wave propagation through the atmosphere, both at radio and optical frequencies: physical and statistical modeling for E.M. propagation applications.

Dr. Lam serves as a Reviewer for IEEE Transactions on Antennas and Propagation and IEEE Antennas and Wireless Propagation Letter.

ABDULLAH M. ALMASOUD received the B.Sc. degree in computer engineering from King Saud University, Riyadh, Saudi Arabia, and the M.Sc. degree in computer engineering and the Ph.D. degree in computer engineering and electrical engineering from Iowa State University, Ames, IA, USA. He is currently an Associate Professor with the Department of Electrical Engineering, Prince Sattam Bin Abdulaziz University, Al-Kharj, Saudi Arabia. His research interests include wireless networks, cognitive radio networks, the Internet of Things, UAV-assisted networking, and RF energy harvesting. He was a recipient of the Best Paper Award from the IEEE Global Communications Conference 2018 on Ad Hoc and Sensors Networks Symposium.